

Optimization of spot welding parameters of stainless steel 304 and 316

Nuri Nasser
Abosag1*

Hamza.K. Jahran1

Faisal Abdussalam
Alfagi3

Nori.abosag@gmail.com

selamgrnah@yahoo.com

Faissel2100sgh@yahoo.com

The Higher Institute of Engineering Technology, Gharyan¹
The Higher Institute of Engineering Technology, Al-Najela – Libya²
The Higher Institute of Engineering Technology-Gharyan³

الملخص

في هذا البحث، تم لحام الفولاذ الأوستينيقي المقاوم للصدأ 304 و 316 بواسطة اللحام المقاومة النقطي، حيث تم دراسة العلاقة بين المتغيرات التيار والزمن وقوة الضغط وتأثيرهم على قوة نقطة شد اللحام وقوة قص نقطة اللحام، بالإضافة الي قياس الصلادة ودراسة البنية المجهرية على طول منطقة اللحام وتأثير الحرارة على التغلغل. من خلال مقارنة قيم التيار والزمن مع القيمة الثابتة لقوة الضغط، ومقارنة قيم القوة والتيار مع القيمة الثابتة للزمن، ومقارنة قيمة التيار مع تبوؤ قيمة قوة الضغط وقيمة الزمن. أشارت النتائج على انه كلما زاد الزمن والتيار انتجت قوة شد عالية للوصلة وبالنسبة لقوة الضغط تكون اقل قيمة.

الكلمات المفتاحية: الفولاذ الأوستينيقي المقاوم للصدأ 304 و 316 ، لحام البقعة بالمقاومة (RSW) ، الصلابة ، اختبار القص واختبار الشد.

ABSTRACT

In this research, austenitic stainless steels 304 and 316 were welded by resistance spot welding (RSW), where the relationship between current, time and pressure variables was studied and their effect on the joint tensile strength and shear strength, as well as the hardness measurement and microstructure along the weld area has been considered, and effect of heat on penetration. By comparing the current and time values with the constant value of the pressure force, comparing the force and current values with the constant value of

time, and comparing the current value with the constant values of the pressure force and the constant time. The results indicated that increasing the time and current gives the highest shear strength and tensile strength of the joint, but the lower pressure force gives the higher shear strength and tensile strength of the joint.

Key words: austenitic stainless steel 304&316, Resistance spot welding (RSW), Hardness, shear test and tensile test.

1. Introduction

In order to create an undamaged joint, resistance spot welding (RSW), a fusion welding technique, and requirements to apply both heat and pressure; the technique can be carried out in several different ways, but spot welding is the most basic. Then a current is fed between the electrodes, resistance to the current's flow causes enough heat to be generated at the interface that melting occurs, a weld nugget forms, and an autogenous fusion weld is created between the plates [1]. Because of their resistance to corrosion, stainless steels are frequently utilized in a variety of industries. In energy-related systems, such as power generation and petrochemical refining systems, welding of stainless steels is crucial, especially the austenitic grades. Due to the problems associated with the fusion zone and the partially-melted zone have been addressed in previous phenomena in stainless steel.

A class of Fe-base alloys known as stainless steels is renowned for its superior corrosion and oxidation resistance. Moreover, a trace quantity of carbon is present, either intentionally added or naturally occurring as an impurity. Based on their structural characteristics, stainless steels can be divided into three main groups: ferrite, martensitic, and austenitic [2]

The resistance generated during spot welding can be attributed to the contact resistance at the electrode-sheet interfaces and sheet faying surface and bulk resistance of the austenitic stainless steel. Contact resistance is strongly influenced by temperature and pressure while bulk resistance changes with only temperature [3]. During the spot welding technique, two constantly cooled electrodes clamp down on two or more worksheets. Afterwards when, the electrodes are subjected to AC or DC current at a low voltage,

allowing fusion to form at the faying surface of the material to be joint [4].

Resistance spot welding of AISI304 requires a relatively lower current range while AISI316 demanded higher currents; Differences in resistivity due to different chemical composition found in stainless steel can result in a reduction of the required currents for welding also shown is the relatively slight welding range for AISI304 compared to AISI316. Hence, AISI304 has a reduced weldability range when compared to AISI316 [5-8].

The purpose of this study is not to examine welds of differing stainless steel materials. On the other hand the study of the effect of different parameters such as current, time, and force on the mechanical properties and microstructure using resistance spot welding for the austenitic stainless steel, AISI304 to AISI316

2. Experimental Work

2.1 Material and Specimen

The materials used in this study are AISI 304 and AISI 316 stainless steel plates with thickness of 2.5mm. The chemical composition are shown in Table1 this was done using Optical Emission Spectrometer at the Libyan higher vocation center for casting, and Table 2 shown the mechanical properties according to The American Iron and Steel Institute (AISI).

Table 1. Chemical Composition of Base Metal (wt %)

B.M	C	Cr	Ni	Mo	Si	Mn	Cu	P	Fe
304	0.07	18.4	8.37	0.12	0.51	0.1.65	0.39	0.03	Balance
316	0.08	17.2	10.1	2.0	0.75	2.0	0.61	0.045	Balance

Table 2. Mechanical Properties.

Materials	Tensile strength (MPa)	Yield strength (MPa)	Elongation %
304	586	241	55
316	579	290	42

There are a number of trial runs carried out to make the weld bead on plates, before going to the actual experiments, basically, these

trial runs were carried out to set the range of the welding process parameters of RSW for conducting the experiment. The working range parameter decided by inspecting the weld bead visually for any visible defects like cracks and porosity, for the upper and lower of control variables.

2.2 Welding Equipment

2.2.1 Resistance Spot Welding Set-up

The RSW samples were produced using a centerline 250-kVA pneumatically operated single phase RSW machine with constant current control and a frequency of 60 Hz. The machine shown in Figure 1 is located at the Libyan higher vocation center for casting, the RSW machine equipped with the Data Acquisition System (DAQ) system. A truncated class 2 electrode with a 6.0 mm face diameter was used as per AWS standards for a 2.5mm to 4.0mm thick sheet [7]. Electrode stabilization was conducted using endurance coupon procedures, which conducted for each new set of electrodes. A Total number of welds per electrode was monitored to stay below the electrode degradation limits. Cooling water flow rate and hold time also followed recommendations of 4 l/min and 5 cycles, respectively.



Figure 1. Centerline AC RSW apparatus

2.2.2 Data Acquisition System

The RSW machine was fully equipped with a data acquisition (DAQ) system capable of recording load (± 0.01 kN), displacement

(± 0.01 mm), current (± 0.1 kA) and voltage (± 0.001 V) simultaneously as a function of time. Figure 2 shows a schematic of the DAQ setup on the AC welder. A linear transducer mounted to the top electrode measures the displacement while a calibrated coil collects the dI/dT , which is conditioned to attain current as a function of time. The load cell located under the bottom electrode measures the force applied by the overhead cylinder. The data acquisition rate was 25,000 points per second (pps). Figure 3 shows the typical DAQ output for a typical single pulse weld which includes the initial force, welding force, welding time and hold time.

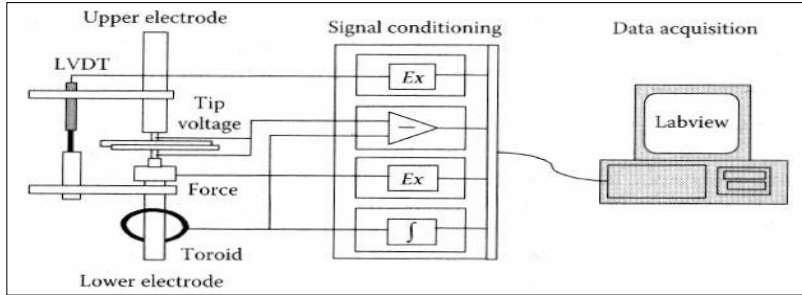


Figure 2. Data acquisition system set-up for resistance spot welding [7]

The energy supplied during RSW is a product of the weld power and time, where the weld power is a product of the measured current (I) and total resistance, where, the total resistance (R_{tot}) is carryout as the summation of the bulk resistances of the two electrodes, bulk resistance of the two sheet metals, and the electrical contact resistance between the interfaces that be welding which assumed to be equal zero.

$$H = I^2 R_{tot} T \quad (1)$$

Where: H = Heat generated (J).

I = Welding Current (A).

R_{tot} = Resistance (ohm).

T = time of current flow (sec).

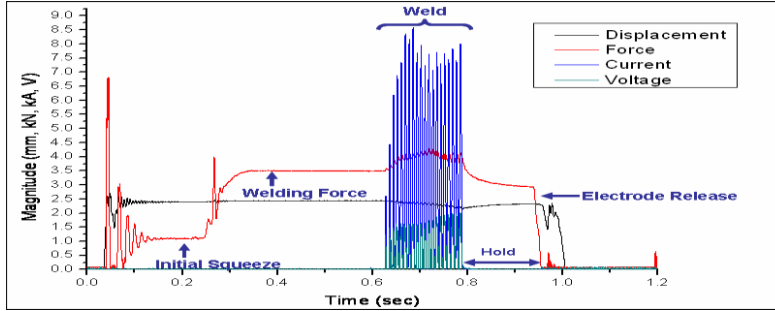


Figure 3. Typical DAQ output for a single pulse weld.

2.3 Samples fabrication and preparation equipment

The samples are cut using Gasparini shear cut machine and Robofil-200 Wire cutting machine as shown in Figure 4 and Figure 5 respectively. After cutting, the sample is mounted with a “phenol powder” using moulding machine Figure 6. This step is necessary to make the samples easier to handle and to protect edges or to reinforce weak or porous material. Buehler's grinding machine was used to carry out the planar grinding. This work has been performed by four types of grinding papers having 240, 600, 800 and 1200 grains size. It is compulsory to start with the paper of the biggest grain size and finish with the finest one. Each step took about 30 seconds. It is important to rotate the sample 90° and wash them carefully between each step. Figure 7 shows the grinding machine used in the study. In order to polish the samples precisely, the polishing process was divided into two parts; Pre-polishing and final polishing. Smooth cloth and lubricant for diamond polishing are used (Diamond suspension; 9μ , 6μ and 3μ). Figures 8a & b show the polishing machine, grinding and polishing disks used in this study respectively. Following the polishing process, a 3% “Nital” (3% HNO_3 in ethanol) etching solution was used as the last phase in the metallographic samples preparation steps. It is necessary to clean again with methanol to avoid marks from the stains. Once metallographic sample preparation has been finished, the samples are ready to perform the macro and micro examination in the microscopy. The etching solution used in this study to reveal the microstructure of stainless steel 304 and 316 before and after the

spot welding process is given as follows 50 ml H₂O + 25 ml HCL + 7.5 g K₃ Fe (CN)₆.

Olympus Optical Microscope model GX51 with digital camera type (Dp70) was used to perform the macro and micro examination as shown in Figure 2-9 Finally, IBER tensile test machine with a maximum power of 6.6KW was also used for tensile tests as depicted in Figure 2-10.



Figure 4. Shear cutting machine



Figure 5. Wire cutting machine



Figure 6. Molding unit



Figure 7. Grinding machine



Figures 8(a). Polishing machine (b) Grinding and polishing disc



Figure 9. Optical microscopes



Figure 10. Tensile test machine

3. Results and Discussion

3.1 Parameter Optimization

RSW samples were produced over a range of force, current, and time parameters. Optimization testing was conducted to determine weld conditions which produced good weld qualities as determined by AWS standards [8-10]. The weld current varied from 6 to 8.2kA, the weld force ranged from 1.5 to 2.5kN, and the weld time was between 20.6 and 20.8 seconds for each samples. The weld samples were subjected to overlap tensile shear testing, U testing, and metallographic examination. A total of 12 tests were conducted per condition including 5 tensile tests, 5 U-tests and 2 samples for metallographic preparation. Optimal welding parameters were attained for tensile shear strength.

Acceptable button diameters were determined by using the AWS relationship for material thickness which is as follows:

$$Mm = 4\sqrt{t} \quad (2)$$

Where Mw (mm) is the minimum nugget diameter and t (mm) is the sheet thickness.

In order to achieve a minimum button size Applying equation 2. The following samples were used to weld 304 and 316 materials.at the time using electrode diameter is 8mm

- Case 1- Austenitic stainless steel 304&316.
- Case 2- Sheet thickness of AISI 304 is 2.5mm.
- Case 3-Sheet thickness of AISI 316 is 2.5mm.

3.2 Mechanical Tests

To measure the mechanical properties of the joint strength, under the effect of three parameters current, time, and force, two tests were done the U-test, and tensile test, as shown in Figure 11 those measurements were done by stabilizing two parameters and changing the third one as following cases:

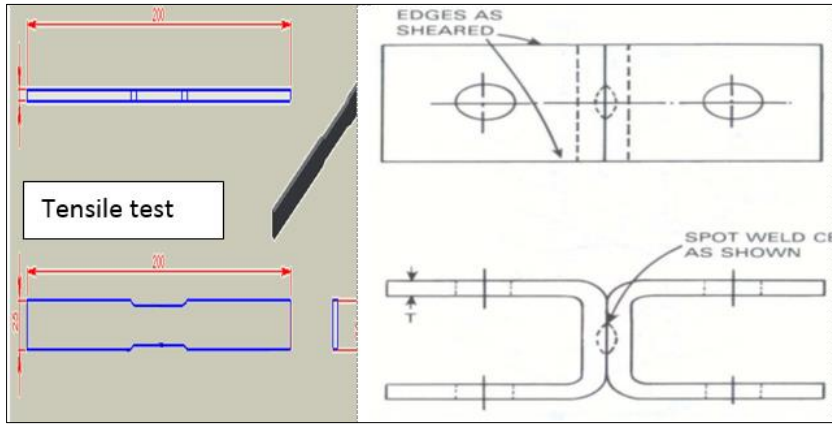


Figure 11. U-test specimen and tensile specimen [7]

Case# 1

In this case, the force was stabilized and time with the following values, force of 1.5kN, and time of 20.6 seconds the current intensity was changed from 60A to 120A as shown in Table 3.

The measured values of joint strength that were obtained using U-test, and tensile test are shown in Figure 12 and 13(a&b) respectively, which are summarized in Table 3.

Table 3. Results of U-test and tensile test

# of sample	Current (A)	U-test (kN)	Tensile test (kN)
1	60	3.5	22.43
2	80	3.6	27.15
3	100	4.3	28.27
4	120	4.9	31.37

The results were obtained from U-test and tensile test are plotted versus the current intensity as shown in Figure 12.

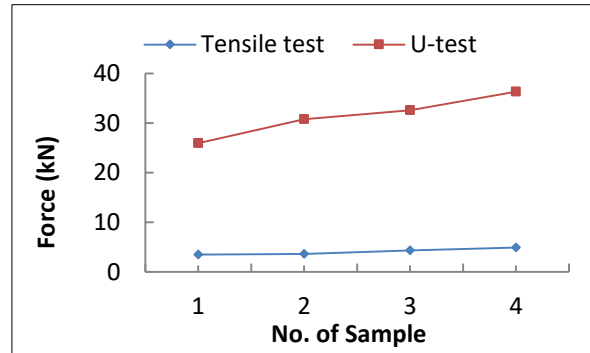
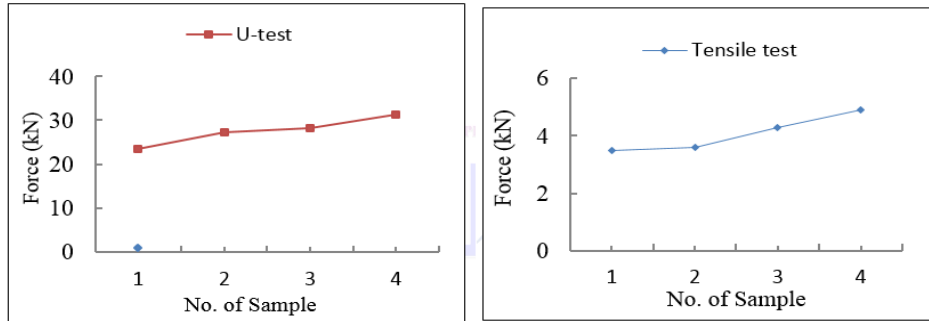


Figure 12. U-test and tensile test results versus the current intensity



Figures 13(a). U-test results versus the current intensity & (b).Tensile test results versus the current intensity

Case# 2

In this case, stabilized force and current with the following values, force of 1.5kN, and current of 80A; and changed the time from 20.5 seconds to 20.8 seconds and the measured values of joint strength that were obtained using U-test, and tensile test, are summarized in Table 4.

Table 4. Results of U-test and Tensile test

# of sample	Time (sec)	U-test (kN)	Tensile test (kN)
5	20.5	6.34	35.40
6	20.6	6.57	35.95
7	20.7	7.04	36.08
8	20.8	7.20	36.20

The results were obtained from U-test and tensile test are plotted versus the welding time as shown in Figure 14 and shown in Figures 15(a & b).

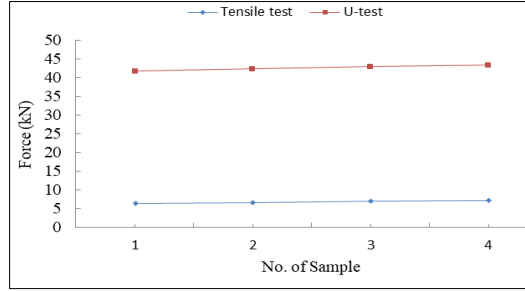
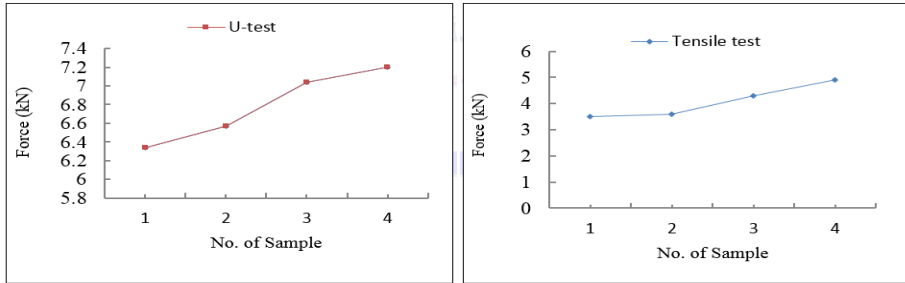


Figure 14. U-test and tensile test results versus the welding time



Figures 15(a). U-test results versus the welding time & (b). Tensile test results versus the welding time

Case# 3

In this case, stabilized current and time with the following values, current of 70 A, and time of 20.7 seconds; and changed the force from 1.5kN to 2.5kN and the measured values of joint strength that were obtained using U-test, and Tensile test, are shown in Table 5.

Table 5. Results of U-test and Tensile test

# of sample	Current (A)	U-test (kN)	Tensile test (kN)
9	1.5	2.99	25.16
10	1.75	1.87	17.84
11	2	1.23	11.25
12	2.5	0.89	9.53

The results were obtained from U-test and tensile test are plotted versus the applied force as shown in Figure 16 and Figures 17(a&b).

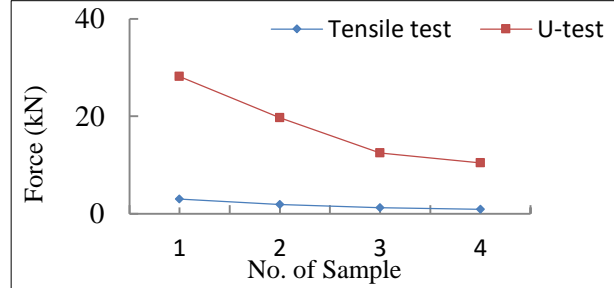
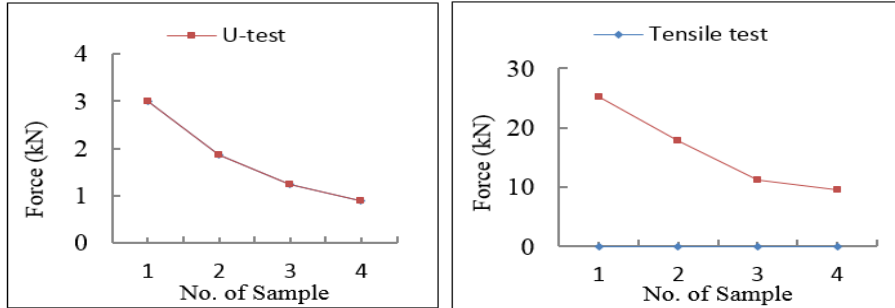


Figure 16. U-test and tensile test results versus the applied force



Figures 17(a). U-test results versus the applied force & (b). Tensile test results versus the applied force

Figures 17 show the representative data for tensile and U-tests conducted on the 304 & 316 alloys. From this data the optimal weld schedule for the joint can be determined. Trends show that failure loads and button diameter increase with weld time and current. However, increasing the welding force generally results in a reduction of failure loads and button diameter. Welds within the upper and lower limits are produced within acceptable current, force and time parameter ranges. Welds below the lower limits have insufficient button diameters, while welds exceeding the upper limit produce expulsion. The optimal welding schedule required for 304 & 316 to produce the maximum failure load (36.08kN) consists of 80 A current, 1.5kN force and a 20.7 sec weld time. Increasing current and time coupled with decreasing weld force results in higher heat generation at the faying interface. From equation 1 it can be

shown that both current and time are proportional to the amount of heat generated during welding. Increasing weld force can reduce contact resistance and hence adversely affect the amount of heat generated. As a result, decreasing welding force increases contact resistance, which generates more heat at the interface. Furthermore, this promotes the formation of larger nuggets and increases bonded area which is reflected in the higher failure loads. Failure loads increase until optimal welding conditions are achieved, after which expulsion can occur. Expulsion typically introduces defects into the weld metal which can include excessive indentation and loss of material.

Table 6. Shows the optimal welding condition attained from weld part testing using welding force, current and time as variables. These conditions produced weldments with the highest tensile shear properties within the part domain. The mechanical properties of welds are displayed in Figure 17. The highest and lowest tensile strengths were attained by 304 & 316.

Table 6. Optimal welding parameters

Welding condition			
304 & 316	Current (Amp)	Force(kN)	Time(sec)
	80	1.5	20.7

3.3 Heat input calculations

Case # 1

Using equation 1 to calculate the heat input ,with fixed value of time of 20.6 seconds, the total resistance of electrodes and sheets of $4.607 \times 10^{-3} \Omega$, and change in the current from 60 A to 120 A, the heat input calculations were summarized in Table 7. The results obtained are plotted as shown in Figure 18.

Table 7. Heat input calculation with change current.

Current (Amp)	Heat input (J)
60	346.33
80	607.39
100	949.04
120	1366.62

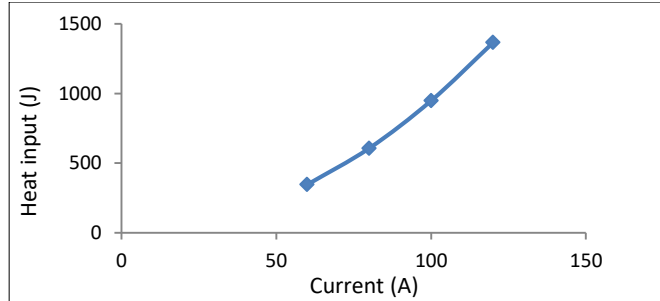


Figure 18. Heat input versus the current

Case # 2

Using equation 1 to calculate the heat input, with the fixed value of Current of 80 A, the total resistance of electrodes and sheets of $4.607 \times 10^{-3} \Omega$, and changing the time from 20.5 to 20.8 seconds, the heat input calculations were summarized in Table 8. The results obtained are plotted as shown in Figure 19.

Table 8. Heat input calculations with change time

Time (seconds)	Heat input (J)
20.5	604.44
20.6	607.39
20.7	610.34
20.8	613.28

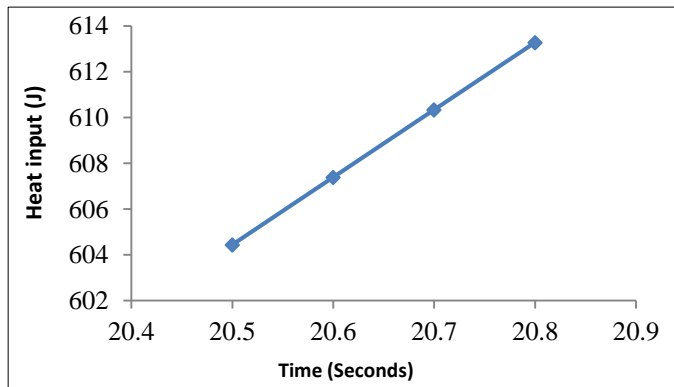


Figure 19. Heat input versus the Time

3.4 Hardness Testing

Primarily, indentation hardness testing is used in engineering and metallurgy. It is usually measured by loading an indenter of specified geometry onto the material and measuring the dimensions of the resulting indentation; by using Brinell test.

According to ASTM E10 standards; the typical test uses a 10mm diameter steel ball as an indenter with a 3000 kP force. For softer materials a smaller force is used, for harder materials, a tungsten carbide ball is substituted for the steel ball. The indentation is measured and hardness is calculated as follows:

$$BHN = \frac{2P}{\pi D(D - \sqrt{D^2 - d^2})} \quad (2)$$

Where: P= Applied force (kP).

D= Diameter of indenter (mm)

d= Diameter of indentation (mm).

The test surface can be quite rough, but a more accurate value is attained with a smoother surface. The hardness testing of the RSW weld data is shown in Table 9 and the relationship between penetration and hardness value in Figure 20.

Table 9. Hardness testing of the RSW weld data

Force (kPa)	D (mm)	d (mm)	H
130	10	2.8	20.69
131	10	2.7	22.45
133	10	1.2	117.17
133	10	3.0	18.38
136	10	3.5	13.69
140	10	1.9	48.94
148	10	2.8	23.55

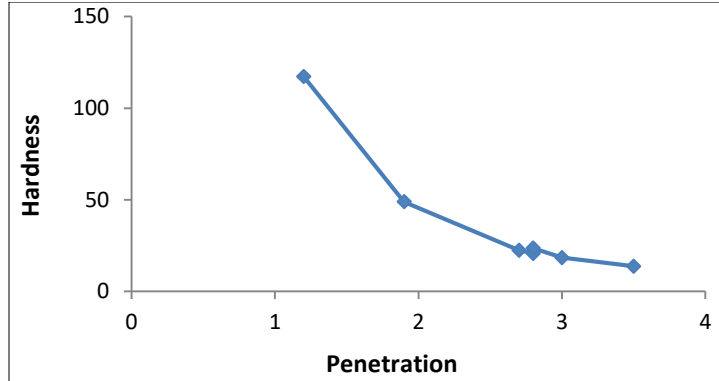


Figure 20. Chart of RSW hardness

3.5 Micro structural Observations

By examining weld cross-sections the different regions including base metal (BM), heat affected zone (HAZ) and fusion zone (FZ) were revealed. Detailed microstructural observations of these regions are shown for each material in Figure 21 and 22 welding parameters used for each material correspond to optimal welding conditions shown in Table 6 to find out the HAZ zone and understand the properties that it presents, an investigation of the microstructure was carried out. The HAZ in spot welding joints may be found by analyzing the hardness curve.

This curve changes severely at the beginning of the HAZ. This is because of the change undergone by the microstructure. The magnification of all the pictures is 100X.



Figure 21. Microstructures in base metal (a)



Figure 21. Microstructures in HAZ (b)

It is possible to see that in HAZ the size of grains becomes larger, this is due to at these points the material having been heated sufficiently long time for grain growth to occur.



Figure 21 (a). Microstructure of AISI304



Figure 22 (b). Microstructure of AISI316

4. Conclusion

In this study the Resistance Spot Welding (RSW) method was used to joint two different sheets of austenitic stainless steel 304 and 316

to produce a good joint strength. The results show several effects which can be summarized as follows:

1. For the changing time value, it was found that better results were obtained for the sample joint with increasing time for welding.
2. When applied a smallest value of pressure force, good joint was obtained.
3. The increasing of the current intensity produced a good joint strength.
4. The optimum welding parameters optioned were current equal 80amp, pressure force equal 1.5KN, and time equal 20.7 sec.

References

- [1]Francisco J. Baldenebro-Lopez, Cynthia D. Gomez-Esparza, Ramon Corral-Higuera," Influence of Size on the Microstructure and Mechanical Properties of an AISI 304L Stainless Steel-a Comparison between Bulk and Fibers "Materials 2015, 8, 451-461.
- [2]Andrea Di Schino "Manufacturing and Application of Stainless Steels" Printed Edition of the Special Issue Published in Metals.
- [3]Beddoes, J.; Parr, J.G. "Introduction to Stainless Steels", 3rd ed.; ASM International: Northeast, OH, 1999.
- [4]Unnikrishnan, Rahul, Satish, K.S.N.; Ismail, T.P." Effect of heat input on the microstructure, residual stresses and corrosion resistance of 304L austenitic stainless steel weldments". Materials Characterization. 2014, 93, 10–23.
- [5]Hao SZ, Wu PS, Zou JX," Microstructure evolution occurring in the modified surface of 316L stainless steel under high current pulsed electron beam treatment "Applied Surface Science Journal 2007; 253(12):5349–54.
- [6]RWMA, "Resistance Welding Manual" 4th edition, 2003.
- [7]Yan MF, Liu RL, Wu DL. Improving the mechanical properties of 17-4PH stainless steel by low temperature plasma surface treatment. Materials and design, April 2010; 31(4):2270–22733.
- [8]Mr. Kumar1, Dr.S.Verma, " Experimental Investigation for Welding Aspects of AISI 304 & 316 by Taguchi Technique for the

- Process of TIG & MIG Welding'. International Journal of Engineering Trends and Technology- Volume2 Issue2- 2011.
- [9]ANSI/AWS/SAE, “Recommended Practices for Evaluating the Resistance Spot Welding Behavior of Automotive Sheet Steel Materials” 1997
- [10] S. P. Tewari, Ankur Gupta, Jyoti Prakash, Effect of welding parameters on the weldability of material, International Journal of Engineering Science and Technology, Vol. 2(4), 2010, pp512-516.
- [11] J.A. Brooks, J. C. Williams, and A.W. Thompson, Microstructural Origin of the Skeletal Ferrite Morphology of Austenitic Stainless Steel Welds, Metallurgical Transactions A volume 14,1983 pp1271–1281